The Insulin-Stimulated Cell Surface Presentation of Low Density Lipoprotein Receptor-Related Protein in 3T3-L1 Adipocytes Is Sensitive to Phosphatidylinositide 3-Kinase Inhibition†

Kerry W. S. Ko,‡ Rita Kohen Avramoglu,‡,§ Roger S. McLeod,‡,|| Jelena Vukmirica,‡,§ and Zemin Yao*,‡,§,⊥

Lipoprotein and Atherosclerosis Group, University of Ottawa Heart Institute, 40 Ruskin Street, Ottawa, Ontario, Canada K1Y 4W7, Department of Biochemistry, Microbiology and Immunology, and Department of Pathology and Laboratory Medicine, University of Ottawa, Canada

Received August 1, 2000; Revised Manuscript Received September 29, 2000

ABSTRACT: The regulation of low density lipoprotein receptor-related protein (LRP) activity by insulin was studied using 3T3-L1 adipocytes. The LRP mRNA and protein expression were independent of differentiation state of the cells and of insulin treatment. In differentiated cells, insulin treatment acutely stimulated the cell surface presentation of LRP (approximately 2-fold) as evidenced by methylamine-activated α_2-macroglobulin binding and by biotinylation of cell surface LRP. The increased cell surface presentation was accompanied by a 39% decrease in LRP level in the low density microsomes. The magnitude of insulin-stimulated cell surface presentation of LRP was similar to that of transferrin receptor but was much less than that of GLUT4. Both the increases in LRP and GLUT4 cell surface presentation upon insulin treatment were abolished by inhibition of phosphatidylinositide 3-kinase. The increased cell surface presentation of LRP was associated with proportionally increased endocytic activity, and the internalization rate constant (K_e) was not decreased by insulin treatment. Thus, insulin treatment most likely stimulates recycling of LRP from an endosomal pool to the plasma membrane, which is regulated in a phosphatidylinositide 3-kinase-dependent manner in 3T3-L1 adipocytes.

The LDL receptor-related protein (LRP),[1] a multifunctional endocytic receptor involved in the binding and uptake of a wide range of ligands, is a large (600 kDa) member of the LDL receptor gene family (*1*). The mature LRP is a heterodimer consisting of the extracellular α-subunit (515 kDa) and the transmembrane *β*-subunit (85 kDa) that are derived from proteolytic cleavage of a single polypeptide chain by furin at the Golgi apparatus (*2*). LRP is ubiquitously expressed and is abundant in the liver (*3*) and neuronal tissue (*4*). In the liver, LRP functions in clearance of protease/inhibitor complexes (*1*) and of apolipoprotein (apo) E-rich lipoprotein (i.e., chylomicron remnant) (*5*). In brain, LRP is shown to interact with apoE (*6*) and *β*-amyloid precursor protein (*7*, *8*), which suggests a role in neuronal outgrowth and possibly in Alzheimer's disease pathogenesis. The physiological role of LRP in adipose tissue is unclear, although there is evidence for function in chylomicron clearance in rats (*9*). Like the LDL receptor, LRP is a type I transmembrane protein that is internalized via clathrin-coated pits and recycles to the plasma membrane through the endosomal compartment (*10*). The cytoplasmic tail of LRP *β*-subunit contains two copies of the NP*X*Y motif, which is thought to act as the sorting signal for rapid internalization of LDL receptor from the cell surface (*11*).

Regulation of LRP activity is complex. Unlike the LDL receptor, expression of the LRP gene is not sensitive to cellular cholesterol levels (*12*) but appears to be responsive to hormones and growth factors. Upregulation of LRP expression by colony-stimulating factor-1 (*13*) and insulin (*14*) was observed in macrophages and was also observed in trophoblasts during differentiation (*15*). In vascular smooth muscle, LRP activity was increased with altered distribution and recycling following treatment with epidermal growth factor or platelet-derived growth factor-BB (*16*). Nerve growth factor treatment increased LRP activity in neuronal cells by stimulating both gene expression and cell surface presentation (*17*). Furthermore, functional expression of LRP at the cell surface depends on the ER resident chaperone protein called receptor-associated protein (RAP) (*18*, *19*).

† This work was supported by Medical Research Council of Canada Grant MT-12931. K.W.S.K. was supported by a Canadian Diabetes Association Fellowship, R.K.A. by a Medical Research Council Studentship, J.V. by an Ontario Government Scholarship for Science and Technology, and Z.Y. by a Medical Research Council Scientist Award.

* Address correspondence to this author. Telephone: (613) 798-5555, ext 8711. Fax: (613) 761-5281. E-mail: zyao@ottawaheart.ca.

‡ University of Ottawa Heart Institute.

§ Department of Biochemistry, Microbiology and Immunology, University of Ottawa.

⊥ Department of Pathology and Laboratory Medicine, University of Ottawa.

|| Current address: Department of Biochemistry, Dalhousie University, Halifax, NS, Canada B3H 4H7

[1] Abbreviations: α_2M*, methylamine-activated α_2-macroglobulin; apo, apolipoproteins; DMEM, Dulbecco's modified Eagle's medium; FBS, fetal bovine serum; LDL, low-density lipoproteins; LDM, low-density microsomes; LRP, LDL receptor-related protein; PAGE, polyacrylamide gel electrophoresis; PBSCM, phosphate-buffered saline with calcium and magnesium; PI, phosphatidylinositide; RAP, receptor-associated protein; SH2, Src homology 2; SDS, sodium dodecyl sulfate.

10.1021/bi001797+ CCC: $20.00
Published on Web 12/23/2000

Insulin has been reported to regulate the endocytic function of LRP in adipocytes, stimulating redistribution of LRP to the cell surface (*20*), and increasing receptor endocytic rate (*9*). This regulation of LRP resembles the regulation of glucose uptake in adipocytes, which increases markedly upon insulin stimulation owing mainly to net translocation of GLUT4 from an intracellular pool to the plasma membrane (*21*). Activation and appropriate targeting of phosphatidylinositide (PI) 3-kinase to intracellular GLUT4-containing vesicles is necessary for the insulin-stimulated GLUT4 translocation and glucose uptake (*22*).

PI 3-kinase consists of an 85-kDa regulatory subunit (p85) containing two Src homology 2 (SH2) domains and one Src homology 3 domain and a 110-kDa catalytic subunit (p110) (*23*). Binding of insulin to its receptor stimulates phosphorylation of insulin receptor substrate proteins, resulting in their binding to the SH2 domain of p85 and activation of p110 (*23*). The activity of PI 3-kinase has been implicated in numerous cellular functions, such as mitogenesis, differentiation, inhibition of apoptosis, cytoskeletal regulation, and vesicle trafficking/secretion (*24*). Inhibitors of PI 3-kinase that abrogate insulin-stimulated cell surface presentation of GLUT4 include the fungal metabolite wortmannin (*25*) and the synthetic compound LY294002 (*26*).

In this study, insulin regulation of LRP was further examined in 3T3-L1 adipocytes. The effects of differentiation and insulin treatment on LRP gene and protein expression were analyzed. Extending the previous observations that insulin stimulates cell surface presentation and activity of LRP in adipocytes (*9*, *20*), we investigated the requirement for PI 3-kinase activity and step(s) within the endocytic pathway regulated by insulin.

EXPERIMENTAL PROCEDURES

Materials. Dulbecco's modified Eagle's medium (DMEM) and fetal bovine serum (FBS) were obtained from Life Technologies Inc. 3-Isobutyl-1-methylxanthine, wortmannin, LY294002, and human holo-transferrin were obtained from Sigma (St. Louis, MO), dexamethasone from Steraloids (Wilton, NH), and insulin from Boehringer Mannheim (Laval, QC). An anti-human LRP polyclonal antibody was a gift of Dr. G. Bu (Washington University), and an anti-GLUT4 (rabbit anti-insulin regulatable glucose transporter) antibody was purchased from East Acres Biologicals (Southbridge, MA).

Cell Culture. The 3T3-L1 preadipocytes were obtained from the ATCC and were maintained in DMEM containing 10% FBS (*27*), with media changes every 2 days. To induce differentiation, 2 days after reaching confluence, cells were cultured in media containing 0.5 mM 3-isobutyl-1-methylxanthine, 0.25 μM dexamethasone, and 175 nM insulin. Two days later, the cells were changed to media supplemented with 175 nM insulin and thereafter were changed every 2 days to media alone. Six to 12 days after differentiation, the cells were cultured in serum-free DMEM overnight prior to experiments. Human primary adipocytes were isolated from reduction mammoplasty samples as previously described (*28*).

Subcellular Fractionation. Preparation of 3T3-L1 adipocyte subcellular fractions was adapted from previously described methods (*29*, *30*). Cells were washed with and collected in 3 mL of ice cold buffer A (250 mM sucrose, 20 mM HEPES, pH 7.4, 1 mM EDTA, and 1 mM PMSF) and were homogenized by 12 strokes through a chilled ball-bearing homogenizer. The homogenate was centrifuged in an SS34 rotor (16000*g*, 20 min, 4 °C), and the resulting supernatant was centrifuged in a TLA 100.4 rotor (48000*g*, 20 min, 4 °C) to obtain the high-density microsome (HDM) pellet. The low-density microsome (LDM) pellet and cytosol were separated by centrifugation of the 48000*g* supernatant (250000*g*, 1.5 h, 4 °C). Both HDM and LDM pellets were resuspended in 150 μL of buffer A.

Plasma membrane was obtained from the 16000*g* homogenate pellet. To do this, the pellet was resuspended in 1 mL of buffer B (20 mM HEPES, pH 7.4, 1 mM EDTA, and 1 mM PMSF) by homogenization with 20 strokes of a Teflon homogenizer, diluted to 9 mL with buffer B, and overlaid atop a 1 mL of 1.12 M sucrose (in buffer B) cushion. The sample was centrifuged in an SW-41 rotor (100000*g*, 1 h, 4 °C), and the plasma membrane band was collected by puncturing the tube wall with a syringe. The collected sample was adjusted to 2 mL with buffer B and centrifuged in a TLA 100.4 rotor (30000*g*, 30 min) to obtain the plasma membrane pellet that was subsequently resuspended in 150 μL of buffer A. The cell debris pellet (presumably the nuclei/mitochondria fractions) was resuspended in 150 μL of buffer A. Each fraction was subjected to immunoblot analysis for LRP and GLUT4. Negligible LRP was associated with cytosol or the nuclei/mitochondria (cell debris) fractions (data not shown).

Immunoblotting. Proteins of the whole cell lysate or the subcellular fractions obtained above were resolved by SDS−PAGE, electrophoretically transferred to nitrocellulose, and visualized with anti-LRP or anti-GLUT4 antibodies using enhanced chemiluminescence as previously described (*31*).

Northern Blot Analysis. Northern blotting was performed as previously described (*32*), and the membranes were probed with a ^{32}P-labeled *Sal*I−*Sst*II fragment (nucleotides 1550−4435) of the human LRP cDNA.

Cell Surface Biotinylation of LRP. Cells were washed with ice-cold PBSCM (PBS, 0.5 mM $CaCl_2$, 1 mM $MgCl_2$) and incubated with 0.5 mg/mL sulfo NHS (*N*-hydroxysuccinimide)-Biotin (Pierce, Rockford, IL) in PBSCM for 1 h on ice. After biotinylation, the cells were washed twice with and collected in 1 mL of PBSCM, 20 mM Tris-HCl, pH 7.4. A Triton X-100 soluble cell lysate was prepared (*31*) and cleared with protein A-bacterial adsorbent (ICN Biomedicals, Costa Mesa, CA) prior to immunoprecipitation of LRP with a polyclonal antibody raised against human LRP (*32*). The immune complexes were absorbed onto protein A-Sepharose (Amersham Pharmacia Biotech, Baie d'Urfé, QC), washed with 1.4% Triton X-100, and dissolved in a sample buffer [10 mM Tris-glycine, pH 8.3, 8 M urea, 2% (w/v) SDS, 10% (v/v) glycerol, and 5% (v/v) mercaptoethanol]. Proteins were resolved by SDS−PAGE (3−8% gels) and transferred to nitrocellulose. Biotinylated LRP was visualized using horseradish peroxidase-conjugated streptavidin (Amersham Pharmacia Biotech) with chemiluminescence detection.

Ligand Binding Assays. Methylamine-activated α_2M (α_2M*) was purified, iodinated, and used for ligand binding assays (4 h, 4 °C) as previously described (*31*). Similarly, human holo-transferrin was similarly iodinated and used at 2.5 and

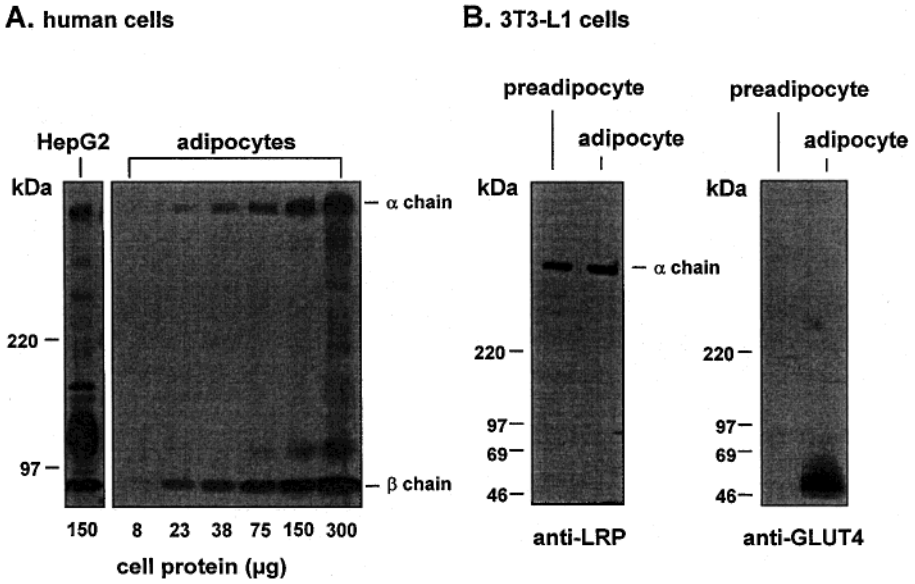

FIGURE 1: Expression of LRP and GLUT4 in adipocytes. (A) Immunoblots of LRP in HepG2 cells and in human primary adipocytes; (B) immunoblots of LRP (left) and GLUT4 (right) in the whole cell lysate of 3T3-L1 preadipocyte and in the differentiated 3T3-L1 adipocytes. Note that while the antibody reacted with both the α- and *β*-chains of LRP in human primary adipocytes, it only reacted with the α-chain in 3T3-L1 cells.

12.5 nM for ligand binding assays (90 min, 4 °C) in the absence and presence of 100-fold excess unlabeled transferrin.

Internalization Assay. The internalization rate constant (K_e) was determined by the In/Sur analysis method of Wiley and Cunningham (*33*) as previously described (*32*).

Ligand Uptake and Degradation Assay. Uptake and degradation of ^{125}I-α_2M* was measured as previously described (*31*).

Effects of Insulin and Wortmannin. Insulin (10 mg/mL in water) and wortmannin (10 mM in DMSO) were stored at −20 °C. Before use, a 174 μM insulin stock was prepared by dilution with 0.01 N HCl. Likewise, a 0.2 mM wortmannin stock was prepared. Appropriate volumes of the diluted solutions were added to media to reach the indicated concentrations. Non-wortmannin treated cells were treated with equivalent volumes of vehicle.

Other Methods. Proteins were determined by the bicinchoninic acid method using BCA reagents (Pierce) according to the manufacturer's instructions.

RESULTS

Expression of LRP in 3T3-L1 Adipocytes. Preliminary immunoblot analysis revealed that the level of LRP expression in human adipocytes was comparable to that in cultured human hepatoblastoma HepG2 cells (Figure 1, panel A). The high level expression of LRP in adipocytes prompted us to investigate its functional role in this specialized cell type. To this end, we used the 3T3-L1 adipocyte model and monitored LRP expression during the cell differentiation. Unlike GLUT4, whose expression in 3T3-L1 cells increased as the cells were differentiated into adipocytes (Figure 1, panel B, right), LRP expression was independent of the differentiation state. Thus, LRP was present both in the preadipocytes and in the fully differentiated adipocytes (Figure 1, panel B, left).

As was the case for LRP proteins, the LRP mRNA was also detected both in the preadipocytes (preconfluent and confluent) and in the differentiated adipocytes (Figure 2, panel A). Treatment of the differentiated cells with insulin for 15, 60, and 720 min had no effect on the LRP mRNA concentrations (Figure 2, panel A, lanes 3−8). In addition, at any time point examined (i.e., 15, 60, and 720 min), the insulin treatment had no effect on LRP protein levels in the differentiated adipocytes (Figure 2, panel B). Thus, like that in human primary adipocytes, the expression of LRP (both protein and mRNA) in 3T3-L1 cells is abundant, and its expression is independent of confluency, differentiation state, or insulin treatment.

Effects of Insulin and Wortmannin on Subcellular Distribution of LRP. Subcellular fractionation of differentiated 3T3-L1 cells was performed (Figure 3) to determine distribution of LRP among LDM, HDM, and plasma membranes. Immunoblotting revealed that the majority of LRP was associated with LDM fraction and plasma membranes (Figure 4, panel A) where GLUT4 was found (Figure 4, panel B). Both GLUT4 and LRP were also associated with the HDM fractions (data not shown). Insulin treatment (100 nM, 10 min) lead to a 39% decrease in LRP recovered in the LDM, while plasma membrane LRP recovery was unchanged (Figure 4, panel A). Under the same conditions, GLUT4 recovery within LDM decreased 49%, which was accompanied by a 250% increase in plasma membrane GLUT4 recovery (Figure 4, panel B). The changes in LRP and GLUT4 subcellular distribution upon insulin treatment were abolished in cells that had been pretreated with wortmannin for 20 min (Figure 4, panel A and B). Neither GLUT4 nor LRP that were associated with HDM fractions was altered by insulin treatment (data not shown). Since total cellular LRP protein levels were unchanged following insulin treatment (Figure 2, panel B), the decrease in LDM-associated LRP (Figure 4, panel A) cannot be explained by protein degradation. Rather, the decrease in LDM-associated LRP was the result of translocation of LRP onto plasma membrane as demonstrated by cell surface biotinylation experiment, which revealed that insulin treatment resulted in an 110%

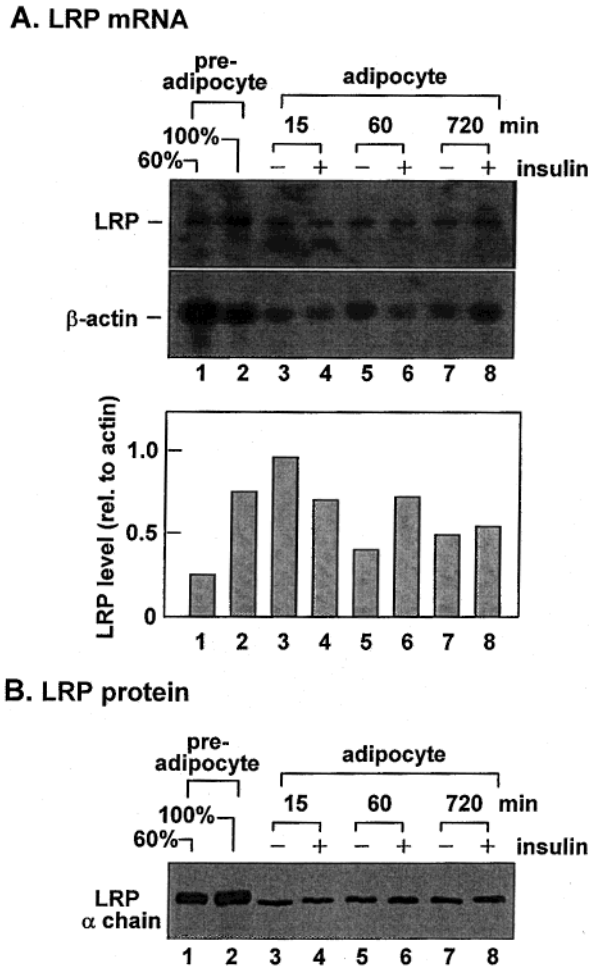

FIGURE 2: Effects of differentiation and insulin on LRP expression in 3T3-L1 cells. (A) Northern blot analysis of LRP mRNA in 3T3-L1 cells at different stages of growth (percentage indicates confluency of preadipocytes) and differentiation or treated with insulin (100 nM) for indicated periods. The experiment was repeated with similar results. (B) Immunoblot analysis of LRP in whole cell lysates (100 μg) of 3T3-L1 cells at different stages of differentiation or treated with insulin (100 nM) for indicated periods.

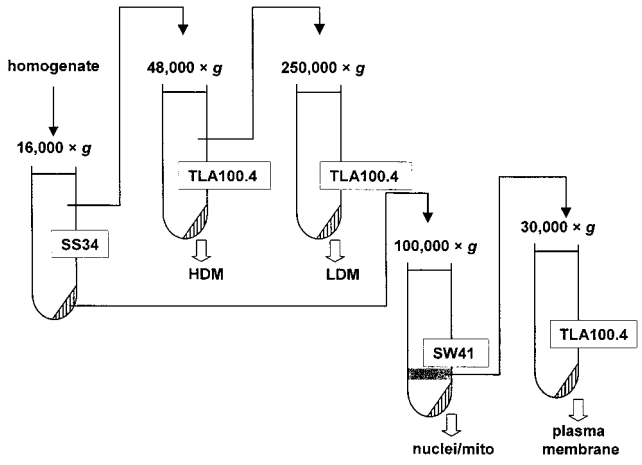

FIGURE 3: Subcellular fractionation of differentiated 3T3-L1 adipocytes. See text for experimental details. HDM, high-density microsomes; LDM, low-density microsomes; mito, mitochondria.

increase in plasma membrane-associated LRP that was sensitive to PI 3-kinase inhibition (Figure 4, panel C). Apparently, the subcellular fractionation technique (Figure 4, panel A) underestimates the degree of translocation (*34*, *35*) and was unable to detect the approximately 2-fold change in plasma membrane LRP upon insulin treatment.

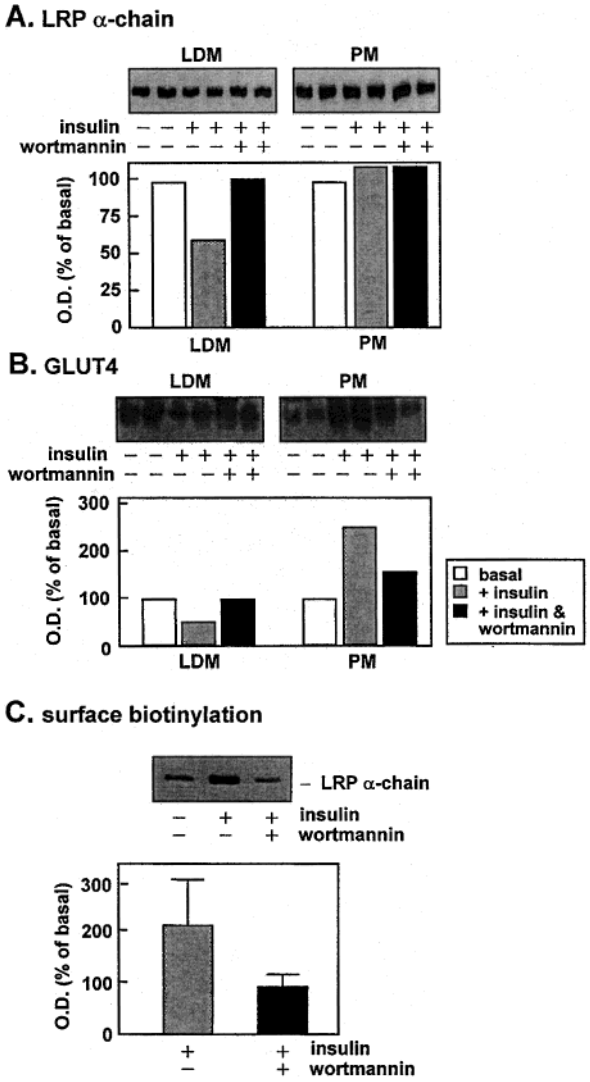

FIGURE 4: Effects of insulin and wortmannin on subcellular distribution of GLUT4 and LRP and cell surface presentation of LRP. (A) immunoblot analysis of LRP associated with LDM fraction and plasma membrane (PM). Differentiated 3T3-L1 adipocytes were treated with insulin (100 nM, 10 min) or/and wortmannin (100 nM, 20 min pretreatment) as indicated, and 40 μg of LDM or PM proteins were resolved by SDS−PAGE and probed with anti-LRP antibody (top). The intensity of the LRP bands was semiquantified by scanning densitometry. Data are presented as percent of basal (i.e., cells treated with no insulin nor wortmannin). (B) immunoblot analysis of GLUT4. The experiment was performed the same as in panel A, except anti-GLUT4 antibody was used. The data are representative of three independent experiments with similar results. (C) cell surface biotinylation of LRP following treatment of adipocytes with insulin or wortmannin as described above. Results from a typical experiment are shown in the fluorograph, while the graph shows scanning densitometry results from three separate experiments (mean ± SD).

The effect of insulin on cell surface presentation of LRP was further demonstrated by ligand binding experiments. Insulin treatment resulted in an 88% increase in specific (RAP-inhibitable) binding of ^{125}I-α_2M* to the differentiated 3T3-L1 adipocyte cell surface, which was abolished by pretreatment with wortmannin (Figure 5, panels A−C). Pretreatment with another PI 3-kinase inhibitor, LY294002 (300 μM) gave the same results as that with wortmannin (data not shown). Thus, measurements of extracellularly

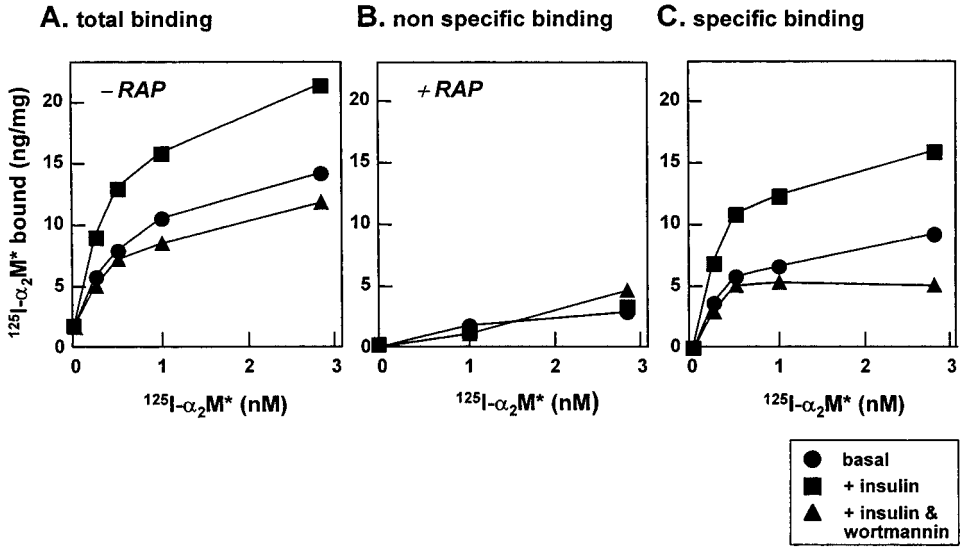

FIGURE 5: Effects of insulin and wortmannin on cell surface LRP ligand binding. (A) total and (B) nonspecific ^{125}I-α_2M* binding to adipocytes at the indicated ligand concentrations, in the absence (A) and presence (B) of RAP (100 nM). (C) Specific binding of ^{125}I-α_2M* was determined from the difference of binding in the presence of RAP from binding in the absence of RAP. Treatments with insulin or wortmannin and insulin were as described in Figure 4.

accessible plasma membrane LRP by biotinylation and studies of ligand binding both suggest that insulin treatment leads to about a doubling of LRP cell surface presentation. Although the magnitude of LRP translocation somewhat differed from that of GLUT4 (approximately 100% versus at least 250%) upon insulin treatment, both pathways appeared to be sensitive to PI 3-kinase inhibition.

Uptake and Degradation of Ligand by LRP. The cell association of ^{125}I-α_2M* to 3T3-L1 adipocytes (i.e., surface bound and internalized) was stimulated by 100% at 30 min and 70% at 1 h upon insulin treatment (Figure 6, panel A). At 2 h (following a lag of 1 h), the rate of degradation of ^{125}I-α_2M* was also stimulated by 70% following insulin treatment (Figure 6, panel B). The magnitude of insulin-stimulated uptake and degradation of ^{125}I-α_2M* (by 70%) was similar to that of increased cell surface presentation (approximately 100%) of LRP. Thus, increased LRP cell surface presentation renders a proportional increase in the rate of LRP endocytosis. The effect of insulin on cell surface presentation of LRP was rapid, reaching maximum in less than 5 min (Figure 6, panel C). These results suggest that insulin-stimulated net translocation of receptors such as LRP to the cell surface provides a mechanism to acutely regulate their endocytic activity.

Internalization Rate of LRP. The effect of insulin and wortmannin, either separately or in combination, on the rate of LRP internalization was determined using the method of Wiley and Cunningham (*33*). In a representative experiment, the ratio of internalized to surface ^{125}I-α_2M* counts (In/Sur) increased linearly with time, permitting determination of the internalization rate constant (K_e) for LRP under the various conditions (Figure 7). Upon insulin treatment, a doubling in cell surface presentation of LRP was accompanied by a 28% increase in K_e (0.212 versus 0.166 min^{-1}, Table 1). Inhibition of PI 3-kinase by wortmannin prior to insulin treatment gave a K_e similar to that in cells treated with insulin alone (0.209 versus 0.212 min^{-1}, Table 1). Thus, the increased LRP cell surface presentation following insulin treatment was not attributable to an inhibition in the rate of LRP internalization. Rather, insulin must stimulate LRP recycling from an intracellular pool to the plasma membrane to bring about an increase in LRP cell surface presentation. It was noted that wortmannin treatment alone resulted in a 25% decrease in K_e as compared to control (0.125 versus 0.166 min^{-1}) accompanied by a 25% drop in cell surface presentation (Table 1). This result suggests that PI 3-kinase activity is probably also involved in the constitutive internalization of LRP under basal conditions.

Other Endocytic Proteins Regulated by Insulin. Insulin treatment resulted in a 60% increase in cell surface presentation of the transferrin receptor, which PI 3-kinase inhibition by wortmannin pretreatment was able to abolish (Figure 8). Thus, the insulin-stimulated cell surface presentation (<2-fold) can be demonstrated for other endocytic proteins. Similar to LRP, treatment of the cells with wortmannin alone lead to a 45% decrease in transferrin receptor at the cell surface as compared to basal levels (Figure 8).

DISCUSSION

The current study is the first to demonstrate that insulin treatment results in an acute physical translocation of LRP from an intracellular pool to the plasma membrane in differentiated 3T3-L1 adipocytes. Combined data from cell surface biotinylation (Figure 4, panel C) and ligand binding (Figure 5) experiments provided unambiguous evidence that the cell surface presentation of LRP is increased by approximately 2-fold by insulin treatment. The current study is also the first to reveal that the insulin-stimulated translocation of LRP from an intracellular pool to the plasma membrane is sensitive to inhibition of PI 3-kinase. Kinetic analysis has shown that the increase in cell surface presentation of LRP is associated with a proportional increase in LRP endocytic activity (Figure 6) and is not attributable to decrease in LRP internalization (Figure 7). This acute regulation of LRP occurred at the posttranslational level, since insulin treatment did not affect either LRP mRNA or cellular protein levels. Other endocytic proteins such as transferrin receptor behave similarly to LRP (Figure 8),

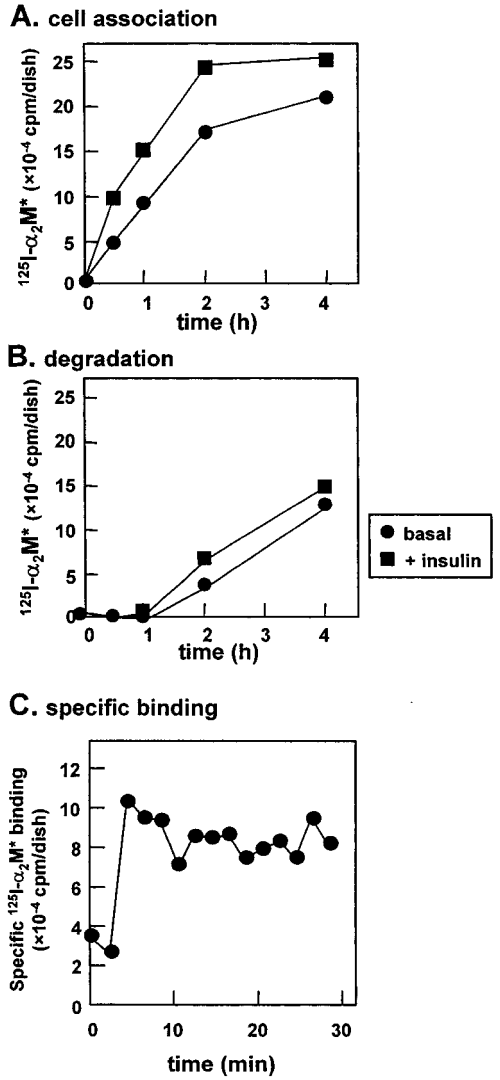

FIGURE 6: Time course of effect of insulin on ligand binding and ligand uptake and degradation by 3T3-L1 adipocytes. (A) Cell association of ^{125}I-α_2M* during incubation of adipocyte with 1 nM ^{125}I-α_2M* at 37 °C for the indicated times. (B) Trichloroacetic acid-soluble, noniodide radioactivity within the media after incubation with ^{125}I-α_2M* at 37 °C for the indicated times. All data (binding, cell association, and degradation) are specific values calculated by subtracting the counts determined with 100 nM RAP. (C) Specific binding of ligand to adipocytes following insulin treatment (100 nM) for the indicated times, followed by ligand binding assays performed on ice for 4 h with 1 nM ^{125}I-α_2M*.

suggesting that insulin may exert a general effect on translocation of proteins from the recycling endosomal compartment to the plasma membranes.

Because the responses of LRP and GLUT4 to insulin bear some similarities, LRP translocation to the plasma membrane can be compared to that of GLUT4. The signaling pathway for insulin regulation of GLUT4 translocation has been investigated extensively. The key steps involved in GLUT4 translocation include activation of insulin receptor substrates and recruitment of PI 3-kinase to the GLUT4-containing membrane compartment (*22*). Although the majority of the intracellular insulin-responsive GLUT4 compartment is recovered within the LDM fraction (*36*), biochemical studies have suggested that some of the GLUT4-containing vesicles may represent separate entities that are kinetically different from the constitutively recycling endosome system (*37*, *38*).

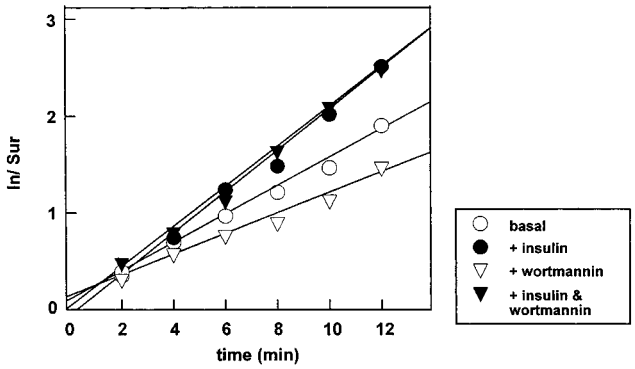

FIGURE 7: In/Sur plot of effect of insulin and wortmannin on internalization of ^{125}I-α_2M*. Cells were labeled with 1 nM ^{125}I-α_2M* (37 °C) and placed on ice at the indicated times. Following Pronase digestion the cell surface (Sur) and internalized (In) counts were quantified to determine the In/Sur ratios. This experiment was repeated with similar results.

Table 1: Internalization Rate Constant (K_e) versus Cell Surface Presentation of LRP

treatment	K_e[a] (min^{-1})	surface presentation[b] (× 10^{-4} cpm/dish)
basal	0.166	7.90
insulin	0.212	15.04
wortmannin	0.125	5.90
insulin + wortmannin	0.209	8.05

[a] The internalization rate constant (K_e) was determined from the slopes of Δ(In/Sur)/Δt (the slope of In/Sur versus time) from Figure 7 for the various treatment conditions. [b] Corresponding measurements of LRP surface presentation under the same treatment conditions were determined by ^{125}I-α_2M* binding at 1 nM as described in Figure 5.

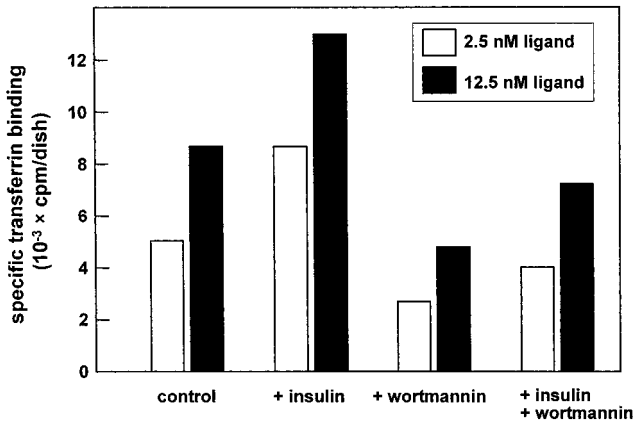

FIGURE 8: Effects of insulin and wortmannin on cell surface transferrin binding. Specific ^{125}I-transferrin binding to adipocytes at the indicated ligand concentrations following treatment of cells with insulin and/or wortmannin as described in Figure 4. This experiment was repeated with similar results.

Our results show that the majority of insulin-responsive intracellular LRP pool also fractionates within the LDM. It remains to be determined if translocation of LRP onto plasma membrane involves the targeting of PI 3-kinase to the endosomal LRP-containing vesicles. If this is the case, then endosomes not only serve as a site for sorting of LRP from its ligands but also act as an LRP storage pool responsive to regulation by insulin through the PI 3-kinase pathway.

A notable difference in insulin-stimulated cell surface presentation is observed between LRP and GLUT4 (Figure 4). The observed modest increase in surface LRP and transferrin receptor is in agreement with reported data (*39*)

and is similar to observations made with other integral membrane proteins such as insulin-like growth factor II/mannose 6-phosphate receptor (*40*), GLUT1 (*41*), and sortilin (*35*). Transport of these membrane proteins from recycling endosomes back to the plasma membrane is thought to occur by bulk membrane flow (*42*). Our data suggest that the enhanced cell surface presentation of LRP (and transferrin receptor as well) may be the result of increased recycling rate of this insulin-sensitive compartment. The apparently high magnitude of GLUT4 translocation to the plasma membrane, on the other hand, may reflect an unusually skewed steady-state distribution of this protein toward an endosome or endosome-related compartments by a specialized retention/sorting system that restricts recycling of GLUT4 under basal conditions (*43*). Hence, upon release of the strict retention of GLUT4 or similarly sorted proteins such as insulin responsive aminopeptidase by insulin, even though such proteins then recycle at similar rates as other endosomal proteins (*44*), there is a resultant high degree of translocation.

The signals that determine the rate of internalization, endosomal transport, and recycling of LRP have not been identified. Recently, it has been shown that the NP*X*Y motifs located within the cytoplasmic domain of LRP are not the dominant endocytosis signals (*45*). The importance of NP*X*Y motifs in LRP recycling remains to be determined. In addition, the β-subunit of LRP has been reported to be phosphorylated upon nerve growth factor treatment, accompanied by altered LRP cell surface presentation (*17*). However, it is not known whether phosphorylation is required for LRP translocation and it remains to be determined whether LRP phosphorylation is altered following insulin treatment. Hence, the elements within the LRP polypeptide that govern both the constitutive and the hormone-sensitive intracellular trafficking of LRP deserve further investigation.

The rate of endocytosis describes a combination of internalization and exocytosis/recycling processes (*46*). It is known that in the case of GLUT4, the increase in steady-state cell surface presentation of GLUT4 upon insulin treatment is brought about by increased exocytosis rate and decreased internalization rate (*37*). However, it should be pointed out that the current study did not measure directly the rate of LRP exocytosis. Rather, the conclusion that insulin stimulates LRP exocytosis/recycling was inferred from experiments where the internalization rate and endocytic function of LRP were determined. That the insulin treatment did not decrease the internalization rate constant (K_e) of LRP (Figure 7) suggests that the increased LRP surface presentation is the result of stimulated exocytosis/recycling, and that the increased LRP cell surface presentation is associated with a proportional increase in ligand uptake and degradation (Figure 6) suggests that LRP internalization is not saturated or inhibited by insulin. Our results indicate that although PI 3-kinase activity is required for the insulin-stimulated exocytosis/recycling, it is not involved in LRP internalization under these conditions.

However, it is interesting to note that PI 3-kinase activity appears to be required for the constitutive internalization of LRP under basal conditions. The observations that treatment with wortmannin alone decreased the internalization rate constant (K_e) of LRP (Table 1) and decreased cell surface presentation for LRP (Table 1) and transferrin receptor (Figure 8) suggest that the PI 3-kinase activity may play a role in basal internalization and recycling of the receptors. A similar effect of wortmannin treatment on transferrin receptor internalization has been observed with chinese hamster ovary derived TRVb-1 cells (*47*). However, other studies suggested that wortmannin treatment increases the internalization of transferrin receptor in association with decreased cell surface presentation in chinese hamster ovary (*48*) and human erythroleukemia K562 (*49*) cells. Unfortunately, the effect of insulin treatment on the receptor internalization rates was not determined in those studies. The current study has demonstrated that the inhibitory effect of wortmannin on LRP internalization rate can be overcome by insulin treatment (Table 1), suggesting that the insulin-responsive mechanism might not be entirely dependent on the PI 3-kinase pathway. The involvement of PI 3-kinase activity in basal and insulin-stimulated internalization and recycling of LRP in adipocytes needs to be further examined.

In conclusion, this study has documented that LRP is highly expressed in adipocytes, and the regulation of LRP in this cell type is mainly at the posttranslational level. Although the physiological significance of high-level expression of LRP in adipocytes remains to be elucidated, the current study is the first attempt to define mechanisms by which LRP surface presentation is regulated by insulin treatment.

ACKNOWLEDGMENT

We thank Xiaohui Zha and Robert J. Brown for helpful discussions and critical reading of the manuscript.

REFERENCES

1. Krieger, M., and Herz, J. (1994) *Annu. Rev. Biochem. 63*, 601−637.
2. Herz, J., Kowal, R. C., Goldstein, J. L., and Brown, M. S. (1990) *EMBO J. 9*, 1769−1776.
3. Moestrup, S. K., Gliemann, J., and Pallesen, G. (1992) *Cell Tissue Res. 269*, 375−382.
4. Bu, G., Maksymovitch, E. A., Nerbonne, J. M., and Schwartz, A. L. (1994) *J. Biol. Chem. 269*, 18521−18528.
5. Willnow, T. E., Sheng, Z., Ishibashi, S., and Herz, J. (1994) *Science 264*, 1471−1474.
6. Holtzman, D. M., Pitas, R. E., Kilbridge, J., Nathan, B., Mahley, R. W., Bu, G., and Schwartz, A. L. (1995) *Proc. Natl. Acad. Sci. U. S. A 92*, 9480−9484.
7. Kounnas, M. Z., Moir, R. D., Rebeck, G. W., Bush, A. I., Argraves, W. S., Tanzi, R. E., Hyman, B. T., and Strickland, D. K. (1995) *Cell 82*, 331−340.
8. Ulery, P. G., Beers, J., Mikhailenko, I., Tanzi, R. E., Rebeck, G. W., Hyman, B. T., and Strickland, D. K. (2000) *J. Biol. Chem. 275*, 7410−7415.
9. Descamps, O., Bilheimer, D., and Herz, J. (1993) *J. Biol. Chem. 268*, 974−981.
10. Lund, H., Takahashi, K., Hamilton, R. L., and Havel, R. J. (1989) *Proc. Natl. Acad. Sci. U.S.A. 86*, 9318−9322.
11. Chen, W. J., Goldstein, J. L., and Brown, M. S. (1990) *J. Biol. Chem. 265*, 3116−3123.
12. Kutt, H., Herz, J., and Stanley, K. K. (1989) *Biochim. Biophys. Acta 1009*, 229−236.
13. Hussaini, I. M., Srikumar, K., Quesenberry, P. J., and Gonias, S. L. (1990) *J. Biol. Chem. 265*, 19441−19446.
14. Misra, U. K., Gawdi, G., Gonzalez-Gronow, M., and Pizzo, S. V. (1999) *J. Biol. Chem. 274*, 25785−25791.
15. Gafvels, M. E., Coukos, G., Sayegh, R., Coutifaris, C., Strickland, D. K., and Strauss, J. F., III (1992) *J. Biol. Chem. 267*, 21230−21234.

16. Weaver, A. M., McCabe, M., Kim, I., Allietta, M. M., and Gonias, S. L. (1996) *J. Biol. Chem. 271*, 24894−24900.
17. Bu, G., Sun, Y., Schwartz, A. L., and Holtzman, D. M. (1998) *J. Biol. Chem. 273*, 13359−13365.
18. Bu, G., Geuze, H. J., Strous, G. J., and Schwartz, A. L. (1995) *EMBO J. 14*, 2269−2280.
19. Willnow, T. E., Armstrong, S. A., Hammer, R. E., and Herz, J. (1995) *Proc. Natl. Acad. Sci. U.S.A. 92*, 4537−4541.
20. Corvera, S., Graver, D. F., and Smith, R. M. (1989) *J. Biol. Chem. 264*, 10133−10138.
21. Rea, S. and James, D. E. (1997) *Diabetes 46*, 1667−1677.
22. Heller-Harrison, R. A., Morin, M., Guilherme, A., and Czech, M. P. (1996) *J. Biol. Chem. 271*, 10200−10204.
23. Shepherd, P. R., Withers, D. J., and Siddle, K. (1998) *Biochem. J. 333*, 471−490.
24. Carpenter, C. L. and Cantley, L. C. (1996) *Curr. Opin. Cell Biol. 8*, 153−158.
25. Ui, M., Okada, T., Hazeki, K., and Hazeki, O. (1995) *Trends Biochem. Sci. 20*, 303−307.
26. Vlahos, C. J., Matter, W. F., Hui, K. Y., and Brown, R. F. (1994) *J. Biol. Chem. 269*, 5241−5248.
27. Frost, S. C., and Lane, M. D. (1985) *J. Biol. Chem. 260*, 2646−2652.
28. Benoist, F., Lau, P., McDonnell, M., Doelle, H., Milne, R., and McPherson, R. (1997) *J. Biol. Chem. 272*, 23572−23577.
29. Clancy, B. M., Harrison, S. A., Buxton, J. M., and Czech, M. P. (1991) *J. Biol. Chem. 266*, 10122−10130.
30. Fisher, M. D., and Frost, S. C. (1996) *J. Biol. Chem. 271*, 11806−11809.
31. Avramoglu, R. K., Nimpf, J., McLeod, R. S., Ko, K. W., Wang, Y., FitzGerald, D., and Yao, Z. (1998) *J. Biol. Chem. 273*, 6057−6065.
32. Ko, K. W., McLeod, R. S., Avramoglu, R. K., Nimpf, J., FitzGerald, D. J., Vukmirica, J., and Yao, Z. (1998) *J. Biol. Chem. 273*, 27779−27785.
33. Wiley, H. S., and Cunningham, D. D. (1982) *J. Biol. Chem. 257*, 4222−4229.
34. Czech, M. P., and Buxton, J. M. (1993) *J. Biol. Chem. 268*, 9187−9190.
35. Morris, N. J., Ross, S. A., Lane, W. S., Moestrup, S. K., Petersen, C. M., Keller, S. R., and Lienhard, G. E. (1998) *J. Biol. Chem. 273*, 3582−3587.
36. James, D. E., Strube, M., and Mueckler, M. (1989) *Nature 338*, 83−87.
37. Pessin, J. E., Thurmond, D. C., Elmendorf, J. S., Coker, K. J., and Okada, S. (1999) *J. Biol. Chem. 274*, 2593−2596.
38. Martin, S., Tellam, J., Livingstone, C., Slot, J. W., Gould, G. W., and James, D. E. (1996) *J. Cell Biol. 134*, 625−635.
39. Davis, R. J., Corvera, S., and Czech, M. P. (1986) *J. Biol. Chem. 261*, 8708−8711.
40. Oka, Y., Mottola, C., Oppenheimer, C. L., and Czech, M. P. (1984) *Proc. Natl. Acad. Sci. U.S.A. 81*, 4028−4032.
41. Calderhead, D. M., Kitagawa, K., Tanner, L. I., Holman, G. D., and Lienhard, G. E. (1990) *J. Biol. Chem. 265*, 13801−13808.
42. Mayor, S., Presley, J. F., and Maxfield, F. R. (1993) *J. Cell Biol. 121*, 1257−1269.
43. Waters, S. B., D'Auria, M., Martin, S. S., Nguyen, C., Kozma, L. M., and Luskey, K. L. (1997) *J. Biol. Chem. 272*, 23323−23327.
44. Subtil, A., Lampson, M. A., Keller, S. R., and McGraw, T. E. (2000) *J. Biol. Chem. 275*, 4787−4795.
45. Li, Y., Paz, M. M., van Kerkhof, P., Strous, G. J., and Bu, G. (2000) *J. Biol. Chem. 275*, 17187−17194.
46. Hao, M., and Maxfield, F. R. (2000) *J. Biol. Chem. 275*, 15279−15286.
47. Li, G., D'Souza-Schorey, C., Barbieri, M. A., Roberts, R. L., Klippel, A., Williams, L. T., and Stahl, P. D. (1995) *Proc. Natl. Acad. Sci. U.S.A. 92*, 10207−10211.
48. Martys, J. L., Wjasow, C., Gangi, D. M., Kielian, M. C., McGraw, T. E., and Backer, J. M. (1996) *J. Biol. Chem. 271*, 10953−10962.
49. Spiro, D. J., Boll, W., Kirchhausen, T., and Wessling-Resnick, M. (1996) *Mol. Biol. Cell 7*, 355−367.

BI001797+